Integrated Modeling of Whole Tokamak Plasma*)

Nobuhiko HAYASHI, Mitsuru HONDA, Kazuo HOSHINO, Kiyotaka HAMAMATSU, Katsuhiro SHIMIZU, Tomonori TAKIZUKA, Takahisa OZEKI and Atsushi FUKUYAMA[1)]

Japan Atomic Energy Agency, 801-1 Mukoyama, Naka 311-0193, Japan

[1)]*Graduate School of Engineering, Kyoto University, Sakyo-ku, Kyoto 606-8501, Japan*

(Received 6 December 2010 / Accepted 4 March 2011)

Development and integration of models for the whole tokamak plasma have progressed on the basis of experimental analyses and first principle simulations. Integrated models of core, edge-pedestal and scrape-off-layer (SOL)-divertor clarified complex and autonomous features of reactor relevant plasmas. The integrated core plasma model including an anomalous transport of alpha particles by Alfven eigenmodes is developed in the core transport code TOPICS-IB and indicates the degradation of fusion performance. The integrated rotation model is developed in the advanced transport code TASK/TX and clarifies the mechanism of alpha particle-driven toroidal flow. A transport model of high-*Z* impurities is developed and predicts large inward pinch in a plasma rotating in the direction counter to the plasma current. TOPICS-IB is extended to include the edge-pedestal model by integrating with the stability code, simple SOL-divertor and pellet models, and clarifies the mechanism of pellet triggered ELM. The integrated SOL-divertor code SONIC is further integrated with TOPICS-IB and enables to study and design operation scenarios compatible with both the high confinement in the core and the low heat load on divertor plates.

Keywords: integrated modeling, tokamak, simulation, transport, stability, core, pedestal, SOL, divertor

DOI: 10.1585/pfr.6.2403065

1. Introduction

In order to realize a steady-state DEMO reactor, researches on advanced tokamak plasmas, characterized by high values of normalized beta, a fraction of self-generated bootstrap current, a confinement enhancement factor and so on, have progressed in JT-60U [1]. In the advanced tokamak plasma, the simultaneous achievement of high performances and its steady-state sustainment are challenging issues, because physical factors are strongly linked with each other. The physics factors include the turbulence, MHD phenomena, wave-particle and plasma-wall interactions and so on, and span over the wide range of the time scale (10^{-10}-10^{3} s) and spatial scale (10^{-6}-10^{2} m). The strong links result in a very complex and self-regulated (autonomous) behavior, which should be understood to predict and control complex and autonomous plasmas in fusion reactors. Numerical simulations help understanding the physics factors behind the links. However, the development of a simulation code including all physics factors with the real time scale and the real spatial scale is a challenging issue. The modeling of various physics and the integration of models for the whole tokamak plasma are one of the most effective methods.

Our strategy of integrated modeling can be explained as follows. First of all, analyses of available experimental data of JT-60U and other devices are being carried out for various kinds of discharges. Additionally, simulations based on the first principle models are being done. Based on results of the experiments and the first principle simulations, new models are developed and integrated into core, edge/pedestal and SOL/divertor codes. These new models and integration are validated by the comparison with the experiments and the first principle simulations.

Four parts of integrated model are being constructed [2–4] toward an integrated code for whole tokamak as shown in Fig. 1. Three main parts are core, edge/pedestal and SOL/divertor regions, and an additional part is the rotation physics which closely relates to both the core and the edge/pedestal regions. The model in the core region includes many important physics factors, which determine high performances, i.e., MHD instabilities such as the resistive wall mode (RWM) and the neoclassical tearing mode (NTM), heat/particle transport caused by collision/turbulence, the formation of internal transport barrier (ITB), the bootstrap current, the current drive and heating by radio-frequency waves and neutral beams (NB), and the interaction between Alfven eigen (AE) mode and alpha particles. The edge/pedestal model is important because it links with physics of the core performance and SOL characteristics, and requires edge transport modeling to form the edge transport barrier (ETB). It also require an analysis of the edge MHD stability causing an edge localized mode (ELM), SOL transports parallel/perpendicular to the mag-

author's e-mail: hayashi.nobuhiko@jaea.go.jp

*) This article is based on the presentation at the 20th International Toki Conference (ITC20).

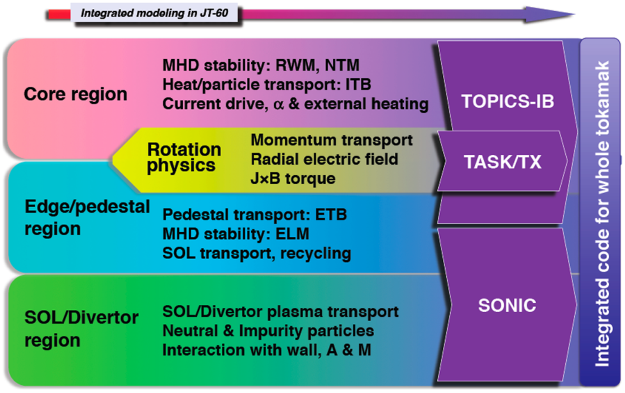

Fig. 1 Strategy of integrated modeling of whole tokamak plasma is that three main parts of integrated models in core, edge/pedestal and SOL/divertor regions and one additional part of rotation physics which closely relates with core and edge/pedestal regions. The integrated models are constructed based on researches of JT-60U experiments and first-principle simulations. Integrated models of core and edge/pedestal regions are built in TOPICS-IB, those of rotation physics are built in TASK/TX and those of edge/pedestal and SOL/divertor region are built in SONIC.

netic field and the recycling at the divertor plate and the wall. In order to study core and edge/pedestal regions, the integrated code TOPICS-IB [5] has been developed on the basis of the 1.5 dimensional (1.5 D) transport code TOPICS [6] extended to the integrated simulations for burning plasma.

Plasma rotation is another important factor affecting the plasma confinement, the ITB/ETB formation and the RWM suppresstion, and its modeling requires the momentum transport, the formation of radial electric field, whose shear can suppress the turbulence, collisional and $\boldsymbol{j} \times \boldsymbol{B}$ torques. To study the rotation physics, the integrated rotation model is developed on the basis of the multi-fluid transport code TASK/TX [7].

The SOL/divertor model is crucial for the establishment of power/particle exhaust control, which is one of the most critical issues in achieving the steady state operation of fusion reactor. The SOL/divertor model consists of transports of SOL/divertor plasmas and of neutrals and impurities, and thus should satisfy many difficult requirements, such as the complex geometry, the atomic and molecular processes of neutrals and impurities. To investigate the SOL/divertor physics, the integrated SOL/divertor code SONIC [8] has been developed by coupling the plasma fluid code SOLDOR [9], the neutral Monte Carlo (MC) code NEUT2D [10] and the impurity MC code IMPMC [11]. The SONIC also can deal with the edge/pedestal region when the core boundary is set inside the edge/pedestal region.

In this paper, integrated core model including the rotation physics are described in Section 2. Development of the integrated model of anomalous transport of alpha particle caused by the AE mode and the resultant reduction of fusion gain are presented. Development of integrated rotation model and the study of mechanism of alpha particle-driven toroidal flow are shown. A pinch model of high-Z impurity in a rotating plasma is presented. Integrated edge/pedestal model are described in Section 3. The mechanism to trigger the ELM by a solid pellet injection is examined. Coupling between TOPICS-IB and SONIC for the whole plasma modeling is described in Section 4. Its application to transient phenomena affecting the whole plasma such as the LH transition is presented. Finally, a summary is given in Section 5.

2. Integrated Core Model Including Rotation Physics

2.1 Integrated model of anomalous transport of alpha particles by Alfven eigen mode

The high confinement of alpha particles is desirable for the high-beta and its sustainment. JT-60U experiments showed that energetic ions were transported from the core region to the outer region due to the resonance interaction between the energetic ions and AE modes [12]. To model the alpha particle transport by AE modes, an integrated model is developed in TOPICS-IB as shown in Fig. 2. For the calculation of alpha particle birth, slowing down process and radial transport, an alpha particle transport code FP-RAT [4, 13] is developed on the basis of Fokker Planck equation of distribution function f on 2D plane (v, r) averaged over the magnetic surface where v and r denote the particle velocity and the minor radius, respectively. The radial particle flux consists of the neoclassical part and the anomalous part. When AE modes arise, the anomalous transport is added into the alpha-particle transport. The anomalous particle flux is assumed as $\Gamma^{\mathrm{AN}} = -D^{\mathrm{AN}}\nabla f^{\mathrm{res}}$. The anomalous diffusivity D^{AN} is assumed as $D^{\mathrm{AN}} = \Sigma_{nm} D_{nm}\gamma_{nm}\Delta_{\mathrm{B}}{}^2/2\exp\{-[(r-r_{nm})/(4\Delta_{nm})]^2\}$ for positive growth rates γ_{nm} of toroidal AE (TAE) modes with the toroidal mode number n and the poloidal mode number m, where the orbit width $\Delta_{\mathrm{B}} = q\rho_{\alpha}$ (q safety factor, ρ_{α} larmor radius of alpha particle), the mode width $\Delta_{nm} = r_{nm}{}^2/(msR)$ (r_{nm} mode location determined by $q(r_{nm}) = (m+1/2)/n$, s magnetic shear, R major radius). The value of D_{nm} is given as a dimensionless parameter, but simulation results shown later do not much depend on D_{nm} when $D_{nm} > 1$. The mode growth rate γ_{nm} is evaluated on the basis of analytical theory [14]. Since a particle is resonated with the modes at the velocity $v_{//} = v_{\mathrm{A}}$ (v_{A} Alfven velocity) and the population of resonant particle decreases with decreasing in v from the birth velocity v_{α}, a part of distribution function resonated with the modes f^{res} is assumed as $f^{\mathrm{res}} \propto \eta(v,r)f$ where $\eta(v,r) = (v^2 - v_{\mathrm{A}}(r)^2)^{0.5}/(v_{\alpha}{}^2 - v_{\mathrm{A}}(r)^2)^{0.5}$ for $v > v_{\mathrm{A}}$, otherwise zero. Figure 3 shows (a) the time evolution of fusion gain Q and a growth rate of $(n,m) = (3,3)$ mode, and (b) profile of

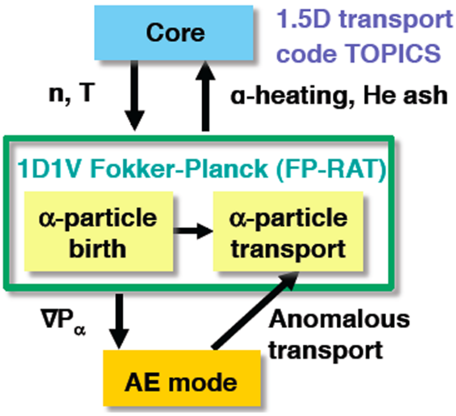

Fig. 2 Schematic flow of integrated calculation of anomalous transport of alpha particles by AE mode.

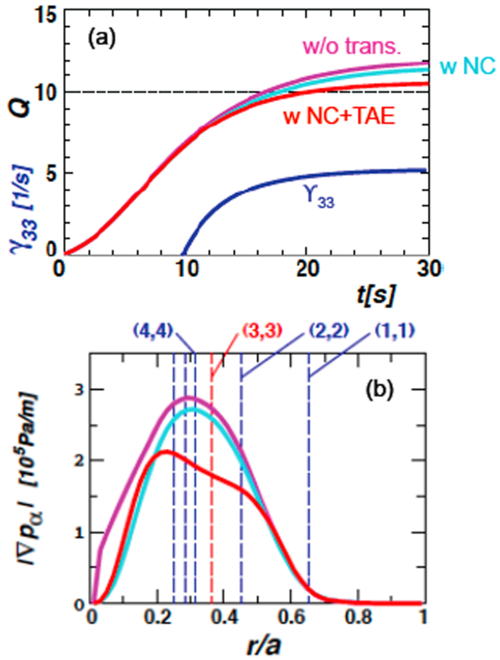

Fig. 3 (a) Time evolution of Q values and a growth rate of $(n,m) = (3,3)$ TAE mode in simulation with parameters of ITER standard scenario for cases without transport, with neoclassical transport (NC) and with anomalous transport by TAE mode in addition to NC (NC + TAE). Growth rate is in case with NC + TAE. (b) Profiles of pressure gradient of α particles at $t = 30\,\mathrm{s}$ for each case in (a) where vertical lines denote locations of TAE modes with numbers (n,m).

pressure gradient of alpha particles at $t = 30\,\mathrm{s}$ for three cases of transport model used in simulations with parameters similar to the ITER standard scenario, i.e., $B_t = 5.2\,\mathrm{T}$, $I_p = 15\,\mathrm{MA}$, $R = 6.3\,\mathrm{m}$, $a = 2\,\mathrm{m}$. In TOPICS-IB, the bulk plasma transport is calculated by a model of current diffusive ballooning mode [15]. A TAE mode with $(n,m) = (3,3)$ is excited from $t = 10\,\mathrm{s}$ in Fig. 3 (a). The anomalous radial diffusion by the TAE mode significantly suppresses the maximum value of alpha particle pressure gradient around $r/a = 0.37$ in Fig. 3 (b). The Q value exceeds

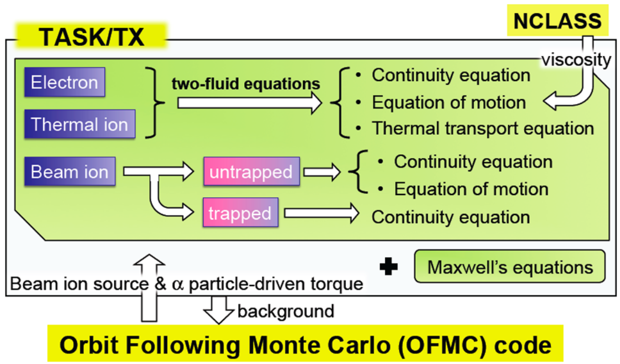

Fig. 4 Schematic illustration of the transport code TASK/TX, which is coupled with neoclassical transport model NCLASS and orbit following Monte Carlo code OFMC.

10 without the anomalous diffusion, but the anomalous diffusion reduces the Q value just above 10 in Fig. 3 (a).

2.2 Integrated rotation model and mechanism of alpha particle-driven toroidal flow

The plasma rotation and its shear play an important role in suppressing the turbulence and MHD instabilities such as RWM, ELM. The active control of ITB strength based on the modification of the radial electric field shear profile by using NB with different directions was successfully demonstrated in JT-60U experiments [16]. Not only RWM but also the energetic particle driven wall mode, which could trigger RWM was not observed in plasmas with the strong rotation [17]. To understand rotation drive mechanisms and its interaction with other physics factors, we are developing the integrated rotation model based on TASK/TX [7] as shown in Fig. 4. Unlike conventional codes, TASK/TX self-consistently solves the continuity equations for all species without imposing the explicit quasi-neutrality condition. Thus, the radial electric field is intrinsically formed to compensate a slight difference between electron and ion movements, and its formation is accurately evaluated in a manner consistent with radial, toroidal and poloidal flows. The neoclassical viscosity is calculated by NCLASS [18]. Profiles of beam ion source and alpha particle-driven torque is evaluated by the OFMC code [19, 20]. This integrated rotation model showed mechanisms of rotation driven by the magnetic-field-ripple loss and the charge separation of fast ions [21, 22].

The mechanism of a torque intrinsically produced by alpha particles and the subsequent possibility to create the toroidal rotation and shear are studied by the integrated rotation model. Figure 5 shows (a) prescribed profiles of safety factor and total pressure in normal magnetic shear (NS) and weakly reversed shear (W-RS) configurations of SlimCS (one of DEMO concepts) [23] and (b) profiles of collisional, $\boldsymbol{j} \times \boldsymbol{B}$ torques and their total calculated by OFMC for prescribed profile in (a). Although alpha par-

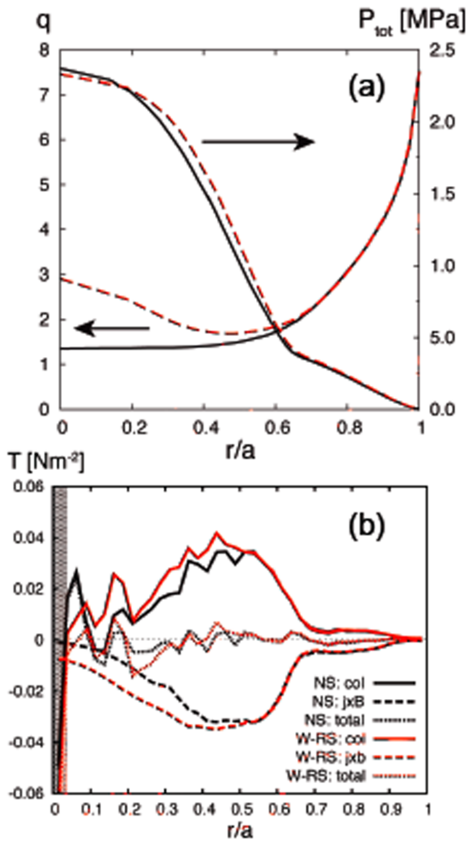

Fig. 5 (a) Prescribed profiles of safety factor and total pressure for NS (solid line) and W-RS (broken line) configurations. (b) Profiles of collisional, $\boldsymbol{j} \times \boldsymbol{B}$ torques, and their total calculated by OFMC for prescribed profiles in (a).

ticles are born isotropically, they have the intrinsic asymmetry in the co- and counter-directions to the plasma current due to the finite orbit width. A source profile of alpha particles is similar to the total pressure profile in Fig. 5 (a) and the gradient of alpha particle source profile is found to produce a co-directed collisional torque and a counter $\boldsymbol{j} \times \boldsymbol{B}$ torque in Fig. 5 (b). From the difference between the NS and W-RS cases in Fig. 5 (b), the magnetic field configuration influences both collisional and $\boldsymbol{j} \times \boldsymbol{B}$ torques. Both torques, however, practically cancel each other out. The resultant total torque is virtually nil and this fact supports the law of conservation of toroidal angular momentum in a case without the loss of alpha particles. For these cases, TASK/TX simulations predict negligibly small toroidal rotation regardless of configuration and the rotation velocity is below the threshold to stabilize RWM [17].

2.3 Pinch model of high-*Z* impurity in rotating plasma

For a plasma facing material in fusion devices, tungsten is one of the most promising candidates with advantages such as the low sputtering yield, the low tritium retention and the high melting point. However, the large radiation loss may occur because the tungsten is not fully ionized even in the core region. The tungsten content in the core region should be reduced for the achievement of ignition condition. JT-60U toroidal rotation scan experiments showed the tungsten accumulation became large as the toroidal rotation increased in the counter direction [24].

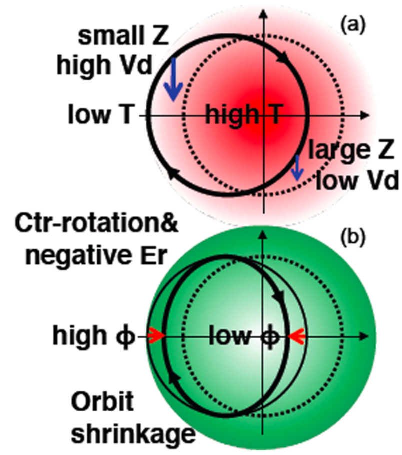

Fig. 6 Schematic mechanisms of (a) inward pinch of high-Z impurity due to atomic process of ionization/recombination and (b) pinch due to effect of radial electric field E_r through Coulomb collisions in case with counter-rotation and negative E_r, where broken lines indicate magnetic surface and thick lines drift orbit. In (a), toroidal drift velocity v_d is inversely proportional to charge number. In (b), thin line corresponds to drift orbit without E_r effect.

For this phenomenon, we model two effects on the transport of high-Z impurity [25, 26]. One effect is atomic processes of ionization and recombination. The mechanism is explained in Fig. 6 (a) as follows; (1) high-Z impurity is accelerated up to a toroidal rotation velocity of background plasma by the friction force, (2) deviation of a drift orbit from a magnetic surface is large, the electron temperature T_e and the charge number Z vary along the drift orbit, (3) the difference of toroidal drift velocity v_d inversely proportional to the charge state causes the inward pinch of high-Z impurity (PHZ). The PHZ velocity v_{PHZ} is analytically derived as, $v_{PHZ} = \{v_{d0}/(2Z_0)\}\{C_T C_{\nabla T}/(C_Z{}^2 + \omega^2)\}$ where the subscript 0 means the initial value, $C_T = \partial\nu/\partial T_e$, $C_Z = \partial\nu/\partial Z$, $\nu = \nu_i - \nu_r$ (difference between the ionization rate ν_i and the recombination rate ν_r), $C_{\nabla T} = dT_e/dr$, $\omega = v/(qR)$, v denote the impurity velocity. The other effect is the radial electric field E_r through the Coulomb collision and its mechanism is explained in Fig. 6 (b) as follows; (1) electric potential ϕ varies along the drift orbit, (2) change in the parallel velocity due to the ϕ variation causes the shrinkage (expansion) of drift orbit in the counter-rotation/negative-E_r (co-rotation/positive-E_r) case, (3) particle moves by the width of shrinkage (expansion) per the Coulomb collision and pinch (unpinch) occurs (here, unpinch means radially outward movement). The E_r pinch (unpinch) velocity is analytically derived as $v_{E_r} = \{[(1-2\alpha)k\mathit{\Delta}_0{}^2]/[2(1-\alpha)^2]\}\{\nu_c/[1+(\nu_c/\nu_b)^2]\}$ where $\alpha = E_r/(B_\theta v_0)$, $k = ZeE_r/(m_Z v_0{}^2)$, $\mathit{\Delta}_0 = v_{d0}/\omega_0$, ν_c denotes the collision frequency, ν_b the poloidal rotation fre-

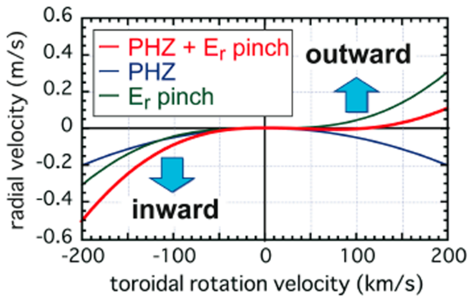

Fig. 7 Radial velocities by inward pinch due to atomic process (PHZ) and by E_r effect as functions of toroidal rotation velocity where total radial velocity is also shown.

quency, B_θ the poloidal magnetic field, m_Z the impurity mass. Figure 7 shows radial velocities v_{PHZ}, v_{E_r} and their sum as functions of toroidal rotation velocity for JT-60U parameters. These radial velocities are validated by a MC code. Both radial velocities are inward and thus the sum of them increases with the counter-rotation, while the radial velocities are opposite and weaken each other in co-rotation. These tendencies are consistent with the JT-60U experiment. This new model needs to be introduced into TOPICS-IB in order to compare the accumulation with experiments.

3. Integrated Edge/Pedestal Model for Study of Pellet Triggered ELM

High pedestal pressure is required to increase the plasma performance, but the energy loss by ELMs is crucial for reducing the divertor plate lifetime. The injection of solid pellets is considered as one method to reduce the ELM energy loss [27]. However, the mechanism to trigger the ELM by the pellet has not yet been clarified.

For the edge/pedestal study, an integrated model is developed in TOPICS-IB [28], in which the transport code TOPICS is coupled with an ideal MHD stability code MARG2D [29], a SOL/divertor dynamic five-point model (D5PM) [30] and the neutral code/model as shown in Fig. 8. The TOPICS simulates the formation of H-mode pedestal by assuming the neoclassical transport in the pedestal region with given pedestal width and the anomalous transport inside the pedestal region. For the ELM model, the stability is examined by MARG2D during the pedestal growth. When the modes become unstable, ELM enhanced thermal/particle diffusivities are added on the basis of eigenfunction profiles with the given maximum value of diffusivities, and maintained for a given time interval. D5PM is based on integral of time-dependent fluid equations. For the density dynamics, the 2D MC code and a simple model, in which a recycling rate is evaluated by the effective mean-free-path of ionization, are used for neutrals in the core and SOL/divertor regions, respectively. This integrated code reproduced the experimentally observed collisionality dependence of ELM energy loss and showed

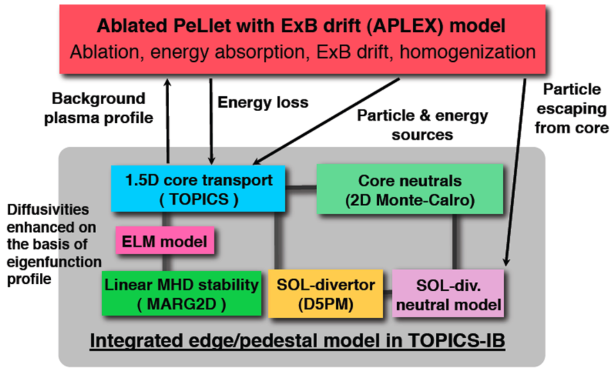

Fig. 8 Integrated edge/pedestal model in TOPICS-IB, in which a transport code TOPICS is coupled with an ideal MHD stability code MARG2D, a SOL/divertor dynamic five-point model, neutral code/model. To study pellet triggered ELM, a pellet model APLEX is also coupled with TOPICS-IB.

that the collisionality dependence is caused by the bootstrap current, the SOL parallel conductive transport and the equipartition effect [28]. The integrtated code also clarified that the steep pressure gradient inside the top of pedestal enhances the ELM energy loss [31], which is validated by the experimental data in JT-60U [32].

To study the pellet triggered ELM, a pellet model APLEX (Ablated PeLlet with $\boldsymbol{E}\times\boldsymbol{B}$ drift) [33] is also coupled with TOPICS-IB as shown in Fig. 8. The APLEX model is based on time-dependent equations of pellet ablation, $\boldsymbol{E}\times\boldsymbol{B}$ drift of plasma cloud detached from the pellet, and cloud energy absorption. We study two mechanisms of pellet triggered ELM on the basis of experimental observations [34], i.e., about 10% decrease in the electron temperature along the pellet penetration path before the density increase, and magnetic perturbation induced by the pellet observed even in L-mode plasmas. First mechanism based on the former observation is that pellet ablation clouds absorbs the energy of background plasma and causes the radial redistribution of pressure due to the subsequent $\boldsymbol{E}\times\boldsymbol{B}$ drift. Second mechanism based on the latter is that the sharp increase in local density and temperature gradients close to an ablated cloud temporarily increase local heat and particle transports in the background plasma. We model these mechanisms and find out if simulation results can reproduce the main experimental observations. Figure 9 shows the time evolution of profiles of (a) total pressure of background plasma and (b) electron diffusivity in a simulation for JT-60U parameters only with the pellet energy absorption effect. The pellet energy absorption produces a region of an increased pressure gradient in the background plasma profile. The local steep pressure gradient within the pedestal can destabilize the high-n ballooning mode ($n > 40$ in this case) and trigger an ELM as shown in Fig. 9. The width of eigenfunction profile is narrower in the pellet triggered ELM than that in "natural" ELMs ($13 \leq n \leq 28$ unstable for about 10% higher

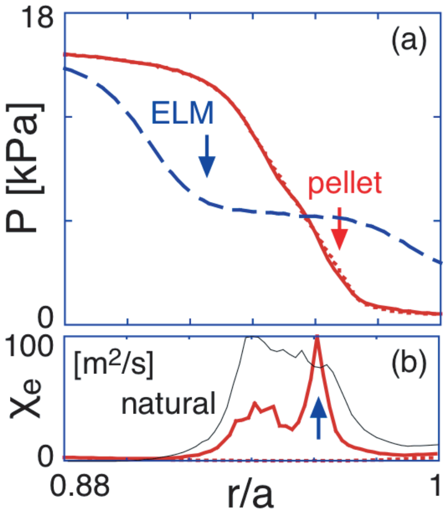

Fig. 9 Time evolution of profiles of (a) total pressure of background plasma and (b) electron diffusivity just before pellet injection (dotted line), at ELM onset (solid line, 0.28 ms after pellet passes separatrix) and after ELM (broken line, ELM duration of 0.2 ms) in a TOPICS-IB simulation only with pellet energy absorption effect. In (b), thin line indicates diffusivity at case of "natural" ELM, which arises for about 10% higher pedestal pressure.

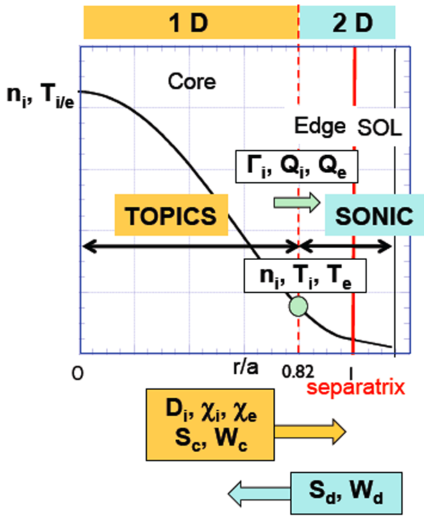

Fig. 10 Schematic illustration of relation between core integrated code TOPICS-IB and SOL/divertor integrated code SONIC.

pedestal pressure). The resultant energy loss is less than half of the "natural" ELMs. Similar results are obtained independently of the pellet injection position. The triggering within the pedestal, the half reduction of ELM energy loss and the independence of injection position agree with experimental observations [27, 34]. On the other hand, the pellet transport enhancement effect is modeled by enhancing the transport for 10 µs following the deposition of each cloud. Simulations show similar results to the case with the pellet energy absorption. Thus, both mechanisms produce a region of an increased pressure gradient in the background plasma profile within the pedestal, which triggers the ELM. When both mechanisms are taken into account, the pellet makes the background pressure perturbation even stronger and triggers the ELM more reliably.

4. Coupling between Core and SOL/Divertor Integrated Models

The feature of integrated SOL/divertor code SONIC composed of SOLDOR, NEUT2D and IMPMC is that the MC approach with the flexibility of modeling is applied to the impurity transport. Additionally, a particle code PARASOL [35] is used to develop kinetic models introduced into SOLDOR and a 3D MC plasma-wall-interaction code EDDY [36] is integrated with SONIC for the self-consistent calculation of physical/chemical sputtering, complex dissociation processes and energy/species dependent reflection. The dynamic evolution of X-point MARFE observed in JT-60U was investigated with SONIC code [37]. It was found that the hydrocarbons sputtered from the dome contribute to the enhanced radiation near the X-point. This kind of simulation, however, was performed by giving the boundary condition of particle and heat fluxes at a certain magnetic surface in the core plasma near the separatrix. Since the core confinement and the SOL/divertor characteristics are significantly affected each other, the above core boundary condition could not be simply given as input parameters. Thus, for the self-consistent analysis of whole plasma, we couple SONIC with the core integrated code TOPICS-IB by the following way.

Figure 10 shows a schematic illustration of relation between TOPICS-IB and SONIC [38]. In the SONIC code, the ion particle flux Γ_i, the ion heat flux Q_i and the electron heat flux Q_e are given on the core edge boundary $r = r_c$ as input parameters. In the present study, $r_c/a = 0.82$ in order to avoid the effect of the significant change in the diffusion coefficient in the H-mode pedestal formed in the region of $0.9 < r/a < 1$. Thus the edge/pedestal region is mainly treated in SONIC. From 1D TOPICS-IB, the fluxes (Γ_i, $Q_{i/e}$) at $r = r_c$ are sent to 2D SONIC, while the plasma quantities (n_i, $T_{i/e}$) at $r = r_c$ are sent to 1D TOPICS-IB from 2D SONIC vice-versa. The 2D MHD equilibrium is relied on the data calculated in TOPICS-IB. Transport coefficients such as particle/thermal diffusivities (D_i, $\chi_{i/e}$) and particle/heat sources (S_c, W_c) from NB and so on are calculated in $r/a < 1$ by TOPICS-IB and used in $r_c/a < r/a < 1$ by SONIC, while particle/heat sources (S_d, W_d) from neutrals and impurities are calculated in $r/a < 1$ by SONIC and used in $r < r_c$ by TOPICS-IB. This integrated code TOPICS-IB/SONIC is executed on the parallel computer. On the parallel computer, the integrated code, which consists of multiple load modules, can be executed with exchanging data between load modules. In order to improve independently each component of the inte-

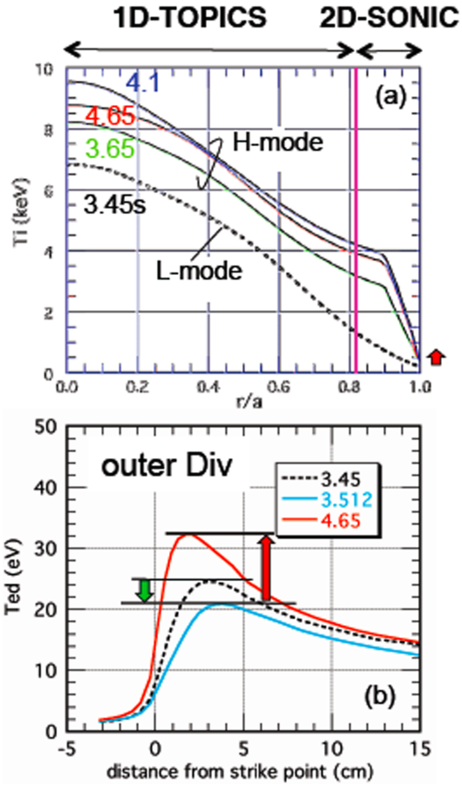

Fig. 11 Time evolution of (a) ion temperature profile inside separatrix and (b) electron temperature profile along outer divertor plate at the LH transition in TOPICS-IB/SONIC coupling simulation.

grated code without interference in each other, we have developed a new MPMD (Multiple Program Multiple Data) computing system [38]. In this system, the grand master PE (processing element) issues commands to control each load module via MPI (Massage Passing Interface). The mutual interface between codes is limited to exchange data through MPI routines. This system realizes easy exchange of modules, ex., TOPICS-IB can be replaced with other transport code such as TASK [39].

In order to demonstrate the advantage of coupling between TOPICS-IB and SONIC, we simulate a series of transient behaviors of an H-mode plasma; the LH transition and the pedestal growth [40]. The simulation is carried out for a high current operation with the lower-single-null configuration of JT-60SA [41] (I_p = 5.5 MA, B_t = 2.3 T, P_{in} = 41 MW). Figure 11 shows the time evolution of profiles of (a) ion temperature inside the separatrix and (b) electron temperature along the outer divertor plate at the LH transition. In the radial profile inside the separatrix, the temperature and density grow up in core and pedestal regions, while the separatix temperature and density is once reduced by the reduction of heat/particle fluxes across the separatrix and gradually increase with the recovery of fluxes due to the growing of temperature/density gradients in the pedestal. On the other hand, in the profile along the divertor plate, peak values of temperature and density are also reduced by the reduction of fluxes and then gradually increase by the recovery of fluxes. The above evolution of profiles inside the separatrix, temperature and density at the separatrix and the divertor plate qualitatively agrees with that in the simulation with the integrated edge/pedestal model in TOPICS-IB in the previous section. The TOPICS-IB/SONIC coupling can simulate the evolution of detailed 2D profiles in edge/pedestal and SOL/divertor regions, and thus enables to study and design operation scenarios compatible with both the high confinement in the core and the low heat load on the divertor plate.

5. Summary

The developments and the integration of models for the whole tokamak plasma have progressed on the basis of experimental analyses and first principle simulations. Integrated models of 1) core, 2) edge-pedestal and 3) SOL-divertor clarified complex and autonomous features of reactor relevant plasmas.

1) The integrated core plasma model including an anomalous transport of alpha particles by AE modes is developed in TOPICS-IB and indicates the degradation of fusion performance by low-n TAE modes in the ITER standard scenario. The integrated rotation model is developed in TASK/TX and clarifies the mechanism of alpha particle-driven toroidal flow. A transport model of high-Z impurities is developed and predicts large inward pinch in a counter-rotating plasma.

2) TOPICS-IB is extended to include the edge-pedestal model by integrating with the stability code, simple SOL-divertor and pellet models, and clarifies the mechanism of pellet triggering ELM.

3) The integrated SOL-divertor code SONIC is further integrated with TOPICS-IB and enables to study and design operation scenarios compatible with both the high confinement in the core and the low heat load on divertor plates.

Success in these consistent analyses of 1), 2) and 3) indicates that the integrated code is an effective means to investigate complex and autonomous plasmas and is expected to help to establish the robust control method for the integrated performance.

Although the integrated code TOPICS-IB/SONIC has the capability to simulate the whole tokamak plasma from the core confinement to the plasma-wall interaction, further development and integration are necessary towards the whole tokamak simulator available even on the desktop of researcher's personal computer so that the researcher can make operation scenarios before experiments in JT-60SA, ITER and DEMO. For the self-consistent rotation study, a simple model will be developed on the basis of TASK/TX and integrated with TOPICS-IB, or the transport solver in TOPICS-IB will be replaced with TASK/TX. Furthermore, we needs to develop models of not only physics parts such as the transport of various Z impurities, but also technical parts such as the external coil current/voltage and the integrated control system for complex and autonomous plasmas. In order to integrate and exchange various codes easily, each codes needs to be modularized on the basis of the common framework, whose definition are being discussed in BPSI (Burning Plasma Simulation Initiative in Japan) [39] and ITER. The application to present and future experiments for physics understanding, the operation scenario development and the model validation is an important issue. Especially, models of high-beta and high-bootstrap-current physics such as RWM, ITB can be validated in JT-60SA experiments, while models of burning physics such as the alpha transport, its related instabilities can be in ITER. The model development and improvement also will be carried out with the progress of first principle simulations especially in high-performance computers such as that in the computer simulation center under the Broader Approach project between EU and Japan. All these efforts can contribute to the development of tokamak simulator applicable to ITER and DEMO.

Acknowledgments

The authors would like to thank all those who have contributed to the JT-60U project. N.H. wishes to express his thanks for valuable discussions, suggestions and efforts to the integrated modeling by JAEA staff and collaborators.

This work was partly supported by the Japan Society for the Promotion of Science, Grant-in-Aid for Scientific Research.

[1] N. Oyama and the JT-60 Team, Nucl. Fusion **49**, 104007 (2009).
[2] T. Ozeki *et al.*, Fusion Sci. Technol. **50**, 68 (2006).
[3] T. Ozeki and JT-60 Team, Phys. Plasmas **14**, 056114 (2007).
[4] N. Hayashi and JT-60 Team, Phys. Plasmas **17**, 056112 (2010).
[5] N. Hayashi *et al.*, Nucl. Fusion **47**, 682 (2007).
[6] H. Shirai *et al.*, Plasma Phys. Control. Fusion **42**, 1193 (2000).
[7] M. Honda and A. Fukuyama, J. Comput. Phys. **227**, 2808 (2008).
[8] H. Kawashima *et al.*, J. Plasma Fusion Res. **1**, 031 (2006).
[9] K. Shimizu, T. Takizuka and H. Kawashima, J. Nucl. Mater. **363**-**365**, 426 (2007).
[10] K. Shimizu *et al.*, J. Nucl. Mater. **313**-**316**, 1277 (2003).
[11] K. Shimizu *et al.*, J. Nucl. Mater. **220**-**222**, 410 (1995).
[12] M. Ishikawa *et al.*, Nucl. Fusion **47**, 849 (2007).
[13] K. Hamamatsu, T. Takizuka, N. Hayashi and T. Ozeki, Proceeding of 11th IAEA Technical Meeting on Energetic particles in magnetic confinement systems, Kyiv, 2009 (IAEA, Vienna, 2010) CD-ROM file.
[14] G.Y. Fu, Phys. Fluids B **1**, 1949 (1989).
[15] A. Fukuyama, K. Itoh, S.-I. Itoh, M. Yagi and M. Azumi, Plasma Phys. Control. Fusion **37**, 611 (1995).
[16] Y. Sakamoto *et al.*, Nucl Fusion **41**, 865 (2001).
[17] G. Matsunaga *et al.*, Phys. Rev. Lett. **103**, 045001 (2009).
[18] W.A. Houlberg, K.C. Shaing, S.P. Hirshman and M.C. Zarnstorff, Phys. Plasmas **4**, 3230 (1997). The NCLASS module is downloaded from http://w3.pppl.gov/ntcc.
[19] K. Tani, M. Azumi, H. Kishimoto and S. Tamura, J. Phys. Soc. Japan **50**, 1726 (1981).
[20] M. Honda *et al.*, "Alpha particle-driven toroidal rotation in burning plasmas", Proc. 23rd IAEA Fusion Energy Conf., Daejeon 2010 (IAEA, Vienna, 2011) CD-ROM file THC/P4-10.
[21] M. Honda, T. Takizuka, A. Fukuyama, M. Yoshida and T. Ozeki, Nucl. Fusion **48**, 085003 (2008).
[22] M. Honda, T. Takizuka, A. Fukuyama, M. Yoshida and T. Ozeki, Nucl. Fusion **49**, 035009 (2009).
[23] K. Tobita *et al.*, Nucl. Fusion **47**, 892 (2007).
[24] T. Nakano, N. Asakura, H. Kubo, J. Yanagibayashi and Y. Ueda, Nucl. Fusion **49**, 115024 (2009).
[25] K. Hoshino, T. Takizuka and T. Nakano, Contrib. Plasma Phys. **50**, 386 (2010).
[26] K. Hoshino *et al.*, "Inward pinch of high-Z impurity due to atomic processes in a rotating tokamak plasma and the effect of radial electric field", Proc. 23rd IAEA Fusion Energy Conf., Daejeon 2010 (IAEA, Vienna, 2011) CD-ROM file THC/P4-12.
[27] N. Oyama, J. Phys. Conf. Series **123**, 012002 (2008).
[28] N. Hayashi *et al.*, J. Phys. Conf. Series **123**, 012025 (2008).
[29] N. Aiba, S. Tokuda, T. Ishizawa and M. Okamoto, Comput. Phys. Commun. **175**, 269 (2006).
[30] N. Hayashi, T. Takizuka and M. Hosokawa, J. Nucl. Mater. **363**-**365**, 1044 (2007).
[31] N. Hayashi *et al.*, Nucl. Fusion **49**, 095015 (2009).
[32] N. Hayashi *et al.*, Nucl. Fusion **51**, 073015 (2011).
[33] N. Hayashi *et al.*, "Integrated simulation of ELM triggered by pellet through energy absorption and transport enhancement", Proc. 23rd IAEA Fusion Energy Conf., Daejeon 2010 (IAEA, Vienna, 2011) CD-ROM file THS/P3-2.
[34] T. Szepesi *et al.*, Plasma Phys. Control. Fusion **51**, 125002 (2009).
[35] T. Takizuka, M. Hosokawa and K. Shimizu, Trans. Fusion Technol. **39**, 111 (2001).
[36] K. Ohya, K. Inai, T. Tanabe and H. Takenaga, J. Nucl. Mater. **363**-**365**, 78 (2007).
[37] K. Shimizu *et al.*, Nucl. Fusion **49**, 065028 (2009).
[38] A. Takayama, K. Shimizu Y. Tomita and T. Takizuka, J. Plasma Fusion Res. SERIES **9**, 604 (2010).
[39] A. Fukuyama, "Integrated Transport Simulation of Burning Plasmas", 2nd ITER International Summer School (Kasuga, Japan, 2008), AIP Conf. Proc. **1095**, 199 (ITOH, S.-I., et al., Ed.) (American Institute of Physics, New York, 2009).
[40] K. Shimizu *et al.*, "Self-consistent integrated modeling of core and SOL/divertor transports and simulation study of transient behavior of heat load on divertor targets", Proc. 23rd IAEA Fusion Energy Conf., Daejeon 2010 (IAEA, Vienna, 2011) CD-ROM file THD/5-2Ra.
[41] Y. Kamada *et al.*, Nucl. Fusion **51**, 073011 (2011).